Molecular Imaging
Volume 15 : 1-10
© The Author(s) 2016
Reprints and permission:
sagepub.com/journalsPermissions.nav
DOI: 10.1177/1536012115624918
mix.sagepub.com
SAGE

Monitoring Apoptosis of Breast Cancer Xenograft After Paclitaxel Treatment With ^{99m}Tc-Labeled Duramycin SPECT/CT

Rui Luo[1], Lei Niu[1], Fan Qiu[1], Wei Fang[2], Tong Fu[1], Ming Zhao[3], Ying-Jian Zhang[4], Zi-Chun Hua[5], Xiao-Feng Li[6], and Feng Wang[1]

Abstract

Our goal was to validate the feasibility of ^{99m}Tc-duramycin as a potential apoptosis probe for monitoring tumor response to paclitaxel in breast cancer xenografts. The binding of ^{99m}Tc-duramycin to phosphatidylethanolamine was validated in vitro using paclitaxel-treated human breast carcinoma MDA-MB-231 cells. Female BALB/c mice ($n = 5$) bearing breast cancer xenografts were randomized into 2 groups and intraperitoneally injected with 40 mg/kg paclitaxel or phosphate-buffered saline. ^{99m}Tc-duramycin (37-55.5 MBq) was injected at 72 hours posttreatment, and single-photon emission computed tomography/computed tomography was performed at 2 hours postinjection. Apoptotic cells and activated caspase 3 in explanted tumor tissue were measured by flow cytometry. Cellular ultrastructural changes were assessed by light and transmission electron microscopy. ^{99m}Tc-duramycin with radiochemical purity of >90% exhibited rapid blood clearance and predominantly renal clearance. The tumor-to-muscle ratio in the paclitaxel-treated group (5.29 ± 0.62) was significantly higher than that in the control. Tumor volume was decreased dramatically, whereas tumor uptake of ^{99m}Tc-duramycin (ex vivo) significantly increased following paclitaxel treatment, which was consistent with apoptotic index, histological findings, and ultrastructural changes. Our data demonstrated the feasibility of ^{99m}Tc-duramycin for early detection of apoptosis after paclitaxel chemotherapy in breast carcinoma xenografts.

Keywords

apoptosis, neoadjuvant chemotherapy, phosphatidylethanolamine, duramycin, tumor response monitoring

Introduction

Active monitoring of the tumor response to treatment is essential for improving the ability to tailor individual therapies and rapidly evaluate novel cancer therapies. The response to treatment is usually assessed by measuring the tumor size with computed tomography (CT) or magnetic resonance imaging.[1] However, there are several fundamental and practical limitations associated with solely employing anatomical measurements as a survival proxy. Tumor shrinkage usually occurs several weeks or months after treatment or it may not occur at all with certain therapies, although the patients show positive responses to treatment.[2] An increased apoptotic index of tumor cells during treatment in preclinical and clinical studies represents a good prognostic indicator.[3-5] On the other hand, a lack of apoptosis could indicate treatment failure. As such, noninvasive imaging of apoptosis provides a potentially valuable approach for evaluating early tumor response in therapies.

The potential use of radiolabeled annexin V has been extensively investigated in noninvasive imaging techniques for

[1] Department of Nuclear Medicine, Nanjing Hospital, Affiliated to Nanjing Medical University, Nanjing, China
[2] Cardiovascular Institute & Fuwai Hospital, Peking Union Medical College & Chinese Academy of Medical Sciences, Beijing, China
[3] Division of Cardiology, Department of Medicine, Feinberg School of Medicine, Northwestern University, Chicago, IL, USA
[4] Department of Nuclear Medicine, Fudan University Shanghai Cancer Center, Shanghai, China
[5] State Key Laboratory of Pharmaceutical Biotechnology, Department of Biochemistry, Nanjing University, Nanjing, Jiangsu, China
[6] Department of Radiology, University of Louisville, Louisville, KY, USA

Submitted: 13/07/2015. Revised: 23/10/2015. Accepted: 29/10/2015.

Corresponding Author:
Feng Wang, Department of Nuclear Medicine, Nanjing Hospital, Affiliated to Nanjing Medical University, 68 Changle Road, Nanjing 210006, China.
Email: fengwangcn@hotmail.com

monitoring tumor response.[6-10] Clinical evaluation has revealed that the binding of radiolabeled annexin V to tumors positively correlates with apoptotic tumor cells obtained from histological analysis.[6] Our previous studies have demonstrated the feasibility of using the ^{18}F-labeled C2A domain of synaptotagmin I for early detection of apoptosis following paclitaxel treatment in not only lung cancer xenografts but also in VX2 rabbit lung cancer.[11,12] However, the relatively large molecular weight, slow blood pool clearance, and biodistribution profiles of these radiotracers severely hampered their potential clinical applications. To overcome these challenges, the use of low-molecular-weight probes provides a suitable alternative to protein-based tracers in monitoring early apoptosis. Peptide-based tracers have rapid clearance from the blood circulation and nontarget tissues in vivo, in addition to efficient diffusion and tissue penetration. In particular, when combined with high-affinity target binding, these favorable pharmacokinetic behaviors will enable the achievement of high-quality imaging data with a low nonspecific background.

Phosphatidylserine (PS) externalization is considered one of the earliest hallmarks of apoptosis. Similar to PS, PE is a constituent of the inner leaflet of the plasma membrane in typical viable cells and becomes externalized to the cell surface during apoptosis.[13-17] Duramycin, which is a lantibiotic peptide, binds to PE with high specificity and affinity.[18-21] The biologic properties of ^{99m}Tc-labeled duramycin such as its favorable uptake and clearance profiles have been documented in several previous quantitative studies,[20-22] and its PE-binding capacity has been shown to be useful for imaging of cell death in other cancer types and tissue injuries.[23,24] Given its low molecular weight, fast clearance kinetics, and high stability, combined with receptor-like binding affinity and specificity, the aim of present study was to evaluate the feasibility of ^{99m}Tc-duramycin as a potential molecular probe for detecting tumor apoptosis following paclitaxel chemotherapy in breast carcinoma xenograft.

Materials and Methods

Reagents and Cell Culture

All other solvents and reagents, unless otherwise stated, were purchased from commercial suppliers and used without further purification. To simplify the process of radiolabeling duramycin, a single-step kit formulation was synthesized. The detailed procedure of the kit formulation has been described previously.[22]

MDA-MB-231 human breast cancer cells were purchased from American Type Cell Culture (ATCC), cultured in Dulbecco modified Eagle medium (Hyclone, Logan, Utah), supplemented with 10% fetal bovine serum (Hyclone) and 100 IU/mL penicillin–streptomycin (Invitrogen, Burlington, Ontario, Canada), and maintained in a humidified 5% CO_2 incubator at 37°C.

^{99m}Tc-Duramycin Radiolabeling

Duramycin is covalently modified with succinimidyl 6-hydrazinonicotinate acetone hydrazone (S-HyNic) and labeled with technetium (^{99m}Tc) using tricine-phosphine coligands. The detailed procedure for the kit preparation has been described previously.[22] Briefly, ~740 MBq (20 mCi) of ^{99m}Tc-Pertechnetate in 500 μL of saline was added to the lyophilized vial of HYNIC-conjugated duramycin, tricine, trisodium triphenylphosphine-3,3′,3″-trisulfonate (TPPTS), and stannous chloride ($SnCl_2$). ^{99m}Tc-pertechnetate ($^{99m}TcO4-$) was obtained from a freshly eluted ^{99}Mo/^{99m}Tc generator. The labeling mixture was heated to 80°C in a lead-lined heating block for 20 minutes. The vial seal was vented with a 25-G needle prior to removal from the heating block and was equilibrated to room temperature before injection.

High-Performance Liquid Chromatography

Quality control procedures, including stability tests, were performed as described previously.[20,22] Radiochemical purity was assayed by reverse-phase radio-high-performance liquid chromatography (HPLC; Integral LC system 100, Japan). The C_{18} column (90 Å pore size, 250 × 4.6 mm) was setup with a buffered mobile phase system consisting of Mobile Phase A (10 mmol/L sodium phosphate, pH 6.8) and Mobile Phase B (100% acetonitrile) at a flow rate of 1.0 mL/min at room temperature. A baseline of 5 minutes at 90% mobile phase A and 10% mobile phase B was followed by a linear gradient to 10% mobile phase A and 90% mobile phase B from 5 to 30 minutes. The level of radioactivity in the eluate was monitored by an in-line gamma counter with an energy window of 140 ± 15 keV.

Stability tests. After labeling, the radiopharmaceutical vials were stored at room temperature for various periods (1, 2, and 4 hours). Subsequently, the radiolabeling mixture in the vials was subjected to radio-HPLC analysis, according to the HPLC method described earlier.

Binding Assay

In the present study, the binding of ^{99m}Tc-duramycin for apoptotic cells was examined as described previously.[22,25] MDA-MB-231 human breast cancer cells were treated with 5 μmol/L paclitaxel to induce apoptosis, and untreated cells served as a control. Cells were centrifuged at 1000 × *g* for 4 minutes and resuspended to a final concentration of 2 × 10^6/mL. Subsequently, cell suspensions were incubated with radiolabeled duramycin (~0.37 MBq) for 5 minutes at room temperature and were washed twice with phosphate-buffered saline (PBS) to remove unbound ^{99m}Tc-duramycin. Finally, 0.5 mL of NaOH was added, and the level of radioactivity was analyzed using a γ-counter with an energy window of 140 ± 15 keV.

Blood Half-Life and Biodistribution in Normal Mice

All animal care and use were performed strictly in accordance with the ethical guidelines and approval of the Nanjing Medical University, Animal Care and Use Committee. Healthy female mice (7 weeks old and weighing 20-22 g) were injected with ^{99m}Tc-duramycin (3.7 MBq/100 μL) via the tail vein. Each group of 3 mice were killed at various time points (5 minutes, 15 minutes, 30 minutes, 1 hour, 2 hours, and 4 hours) by cervical dislocation. Main

organs such as the heart, liver, spleen, lung, kidney, and stomach were quickly removed and weighed carefully. Blood samples were also collected. The radioactivity present in these tissues was measured using a γ-counter (GC-1200, Gamma Radioimmunoassay Counter; USTC Chuangxin Co Ltd, China), and the results are expressed as the mean ± standard deviation (SD) of the percentage of the injected dose per gram of tissue (%ID/g). All radioactivity measurements were corrected for decay.

MDA-MB-231 Tumor-Bearing Model and ^{99m}Tc-Duramycin Ex Vivo Distribution

Female Balb/c nude mice (5 weeks old and weight 20-22 g) were purchased from Beijing Animal Center and housed under environmentally controlled conditions (22°C; 12 hour–12 hour light–dark cycle with the light cycle from 6:00 to 18:00 and the dark cycle from 18:00 to 6:00) and were provided with pathogen-free food and water. MDA-MB-231 human breast cancer cells were cultured as described previously, and 5×10^6 cells in 100 μL of PBS were injected into the mid-right flank of the mice, which developed tumors in approximately 3 weeks. The mice were euthanized when the tumor volume reached a volume of approximately 75 to 100 mm^3.

Mice were randomized into 2 groups (5 mice per group) and intraperitoneally injected with either PBS (nontreated group) or 40 mg/kg paclitaxel (treated group). Both groups were injected with ^{99m}Tc-duramycin (3.7 MBq/100 μL) via the tail vein. All mice were killed after 2 hours by cervical dislocation. Tumor and muscle in each mouse were quickly removed and weighed, the radioactivity in tumor and muscle was measured with a γ-counter, and the data were expressed as the mean ± standard deviation (SD) of the percentage of the injected dose per gram of tissue (%ID/g). All radioactivity measurements were corrected for decay.

Single-Photon Emission Computed Tomography/Computed Tomography Imaging

MDA-MB-231 xenografts were randomized into 2 groups (5 mice per group) and were intraperitoneally injected with either PBS (control group) or 40 mg/kg paclitaxel. Subsequently, ^{99m}Tc-duramycin (37-55.5 MBq) was injected via the tail vein at 72 hours after PBS or paclitaxel treatment. Single-photon emission computed tomography/computed tomography (SPECT/CT) images were acquired on a Nano SPECT/CT scanner (Bioscan, Inc. USA) at 2 hours postinjection, with an energy window of 140 ± 15 keV. The matrix size of the SPECT projections was 256 × 256 (30 s/frame). Briefly, mice were anesthetized with 1% to 2% isoflurane and imaged in a prone position. Static planar images with a frame size of 256 × 256 were acquired for 45 minutes. The images were processed using In Vivo Scope software (Bioscan). For data analysis, regions of interest (ROIs) were drawn over tumors and contralateral normal muscle tissues. Tumor-to-muscle (T/NT) ratios were calculated. Tumor volume was calculated at the same time on day 0, day 3, day 5, and day 7, according to the following equation: tumor volume = 1/2 (length × $width^2$). The mice were killed, and tumor tissues were excised immediately after the imaging experiments for radioactivity measurements and histopathology analysis. The radioactivity uptake was expressed as a percentage of the injected dose per gram of tissue (%ID/g) with the mean ± SD. Subsequently, explanted tumor tissues were subjected to flow cytometry, Terminal-deoxynucleoitidyl Transferase Mediated Nick End Labeling (TUNEL) assay, and transmission electron microscopy (TEM).

TUNEL Staining of Tumor Tissue Sections

Tumor tissue sections (5 μm thickness) were prepared and stained with hematoxylin and eosin (H&E) according to standard protocols and then assessed for apoptosis. In situ cell death was determined by TUNEL staining of tumor tissue sections (paclitaxel-treated and nontreated human breast carcinoma tissues). The TUNEL assay was performed in accordance to the manufacturer's instructions (in situ cell death detection kit; catalog # G3250, Roche Applied Science, Germany) to demonstrate DNA fragmentation.

Ultrastructural Morphology Analysis With TEM

Cell ultramorphology were obtained using a TEM (JEM-1010, Jeol Korea Ltd, South Korea) as described previously. Briefly, the tumor tissues were fixed with 2.5% glutaraldehyde at 4°C, dehydrated with graded ice-cold ethanol (70%, 80%, 90%, and 100%), and embedded in epoxy resin (EPON 812, Serva Feinbiochemica Heidelberg, Corporation. New York, USA). The blocks were cut into ultrathin sections using an ultramicrotome and stained with uranyl acetate/lead citrate.

Flow Cytometry Analysis

Bivariate fluorescein isothiocyanate (FITC)-Annexin V/propidium iodide (PI) analysis was used to detect apoptotic tumor cells in suspension using flow cytometry. Briefly, 10 μL of FITC-Annexin V and 5 μL of PI were added to 200 μL of freshly collected cells suspended in binding buffer at a density of 5×10^5 cells/mL. The cells were incubated at room temperature in the dark for 15 minutes, rinsed in binding buffer, resuspended in 200 μL of binding buffer for 5 minutes on ice, and analyzed by flow cytometry.

To analyze the tumor apoptosis induced by paclitaxel, in addition to FITC-Annexin V/PI staining, activated caspase 3 level was also determined in dissociated tumor cells by flow cytometry using a commercial kit (CaspGLOW™ Fluorescein Active Caspase-3 Staining Kit. BioVision, Inc. USA) according to the manufacturer's protocol. Caspase 3 is an effector caspase that plays a critical role in the execution phase of apoptosis; the present study utilized the caspase inhibitor, DEVD-FMK, conjugated with FITC as a marker for direct determination of activated caspase 3. Briefly, fresh tumor tissues were dissected into small pieces, 1 μL of FITC-DEVD-FMK was added to 300 μL of each sample cell suspension (3×10^5 cells), and the mixture was incubated for 30

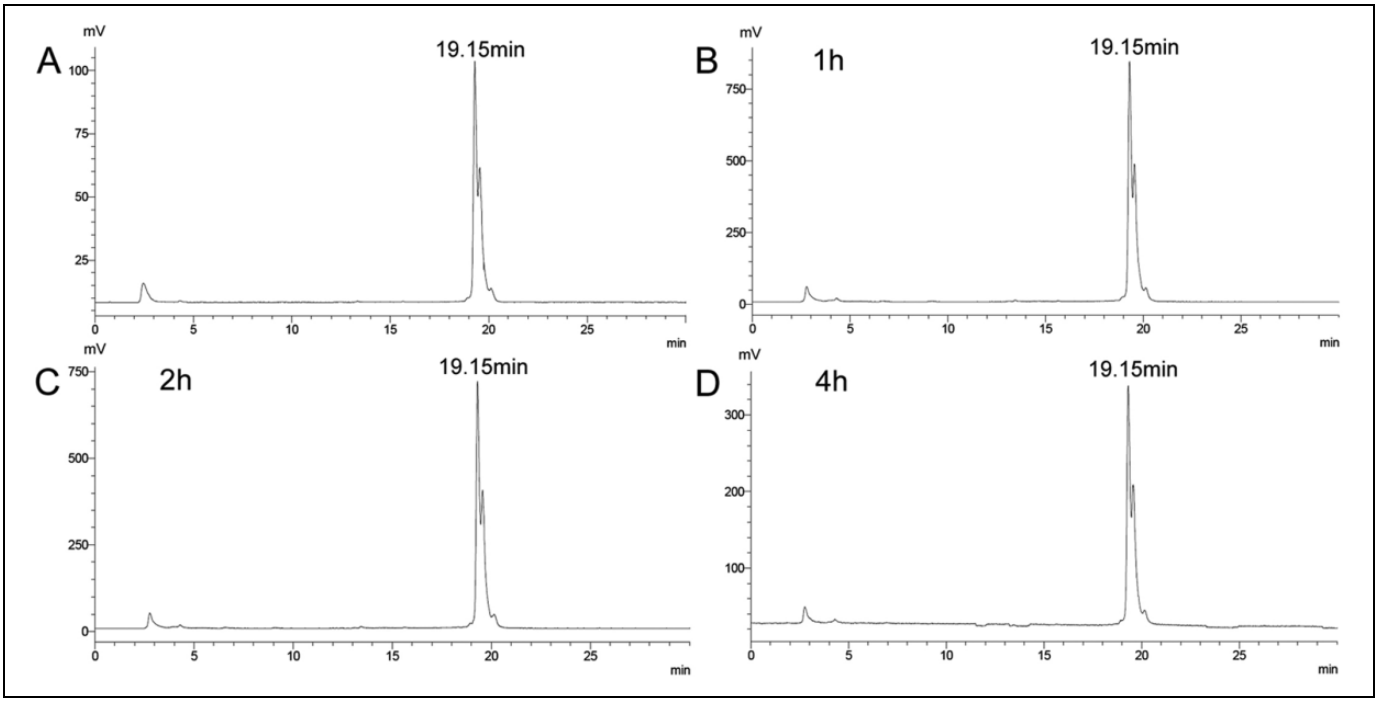

Figure 1. Radio-high-performance liquid chromatography (HPLC) analysis of ^{99m}Tc-duramycin radiolabeling efficiency and in vitro stability at 0 minute (A), 1 hour (B), 2 hours (C), and 4 hours (D). The retention time was 19.15 minutes.

minutes at 37°C in a 5% CO_2 incubator. The supernatant was discarded following centrifugation. Cell suspension was analyzed by flow cytometry. Fluorescence-activated cell sorting analysis was performed on the FL-1 channel with CellQuest software (Becton, Dickinson and Company. USA), and the fluorescence intensity was calculated by gating on live cells.

Statistical Analysis

SPSS 19.0 software (SPSS Inc, Chicago, Illinois) was utilized for statistical analysis. All data are expressed as the mean percentage ± standard deviation (SD). For statistical analysis, Student *t* test was performed. Differences at a 95% confidence level ($P < .05$) were considered significant.

Results

Radiolabeling and Quality Control

The radiochemical purity of ^{99m}Tc-duramycin as determined by radio-HPLC was found to be >90%, with a retention time of 19.15 minutes. ^{99m}Tc-duramycin was found to be stable without significant presence of dissociated radioactivity till 4 hours after radiolabeling, as shown in Figure 1.

Radiotracer Uptake Levels in Treated and Nontreated MDA-MB-231 Carcinoma Cells

The radioactivity uptake in paclitaxel-treated MDA-MB-231 human breast carcinoma cells was 2.23 ± 0.32 fold than that in the nontreated cells ($P < .01$), as seen in Figure 2A. These

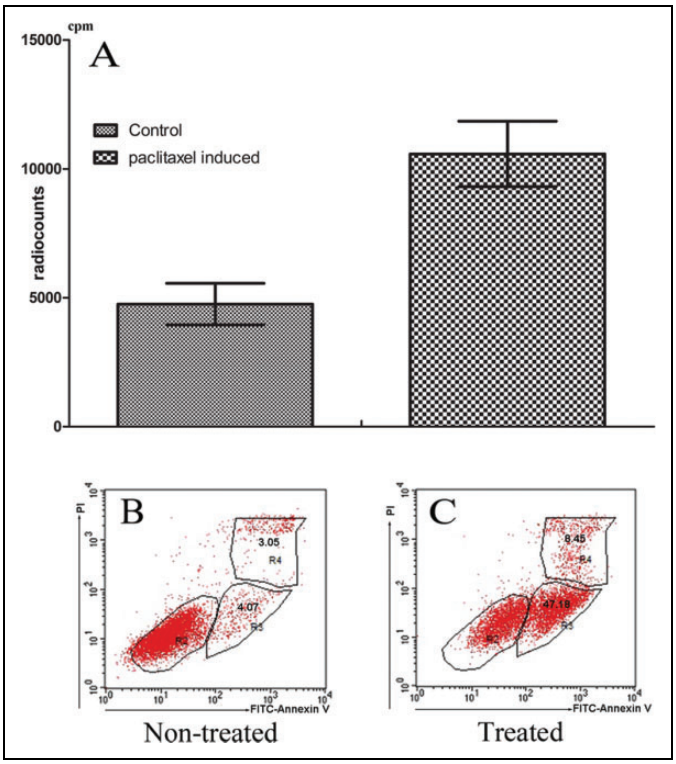

Figure 2. A-C, Radiouptake in treated and untreated MDA-MB-231 breast carcinoma cells (A). Significantly higher radiouptake was observed in paclitaxel-treated MDA-MB-231 cells (2.23 ± 0.32-fold) than in untreated cells. As depicted in (B and C), apoptotic cells were clearly detected in the bivariate fluorescein isothiocyanate (FITC)-annexin V/PI analysis.

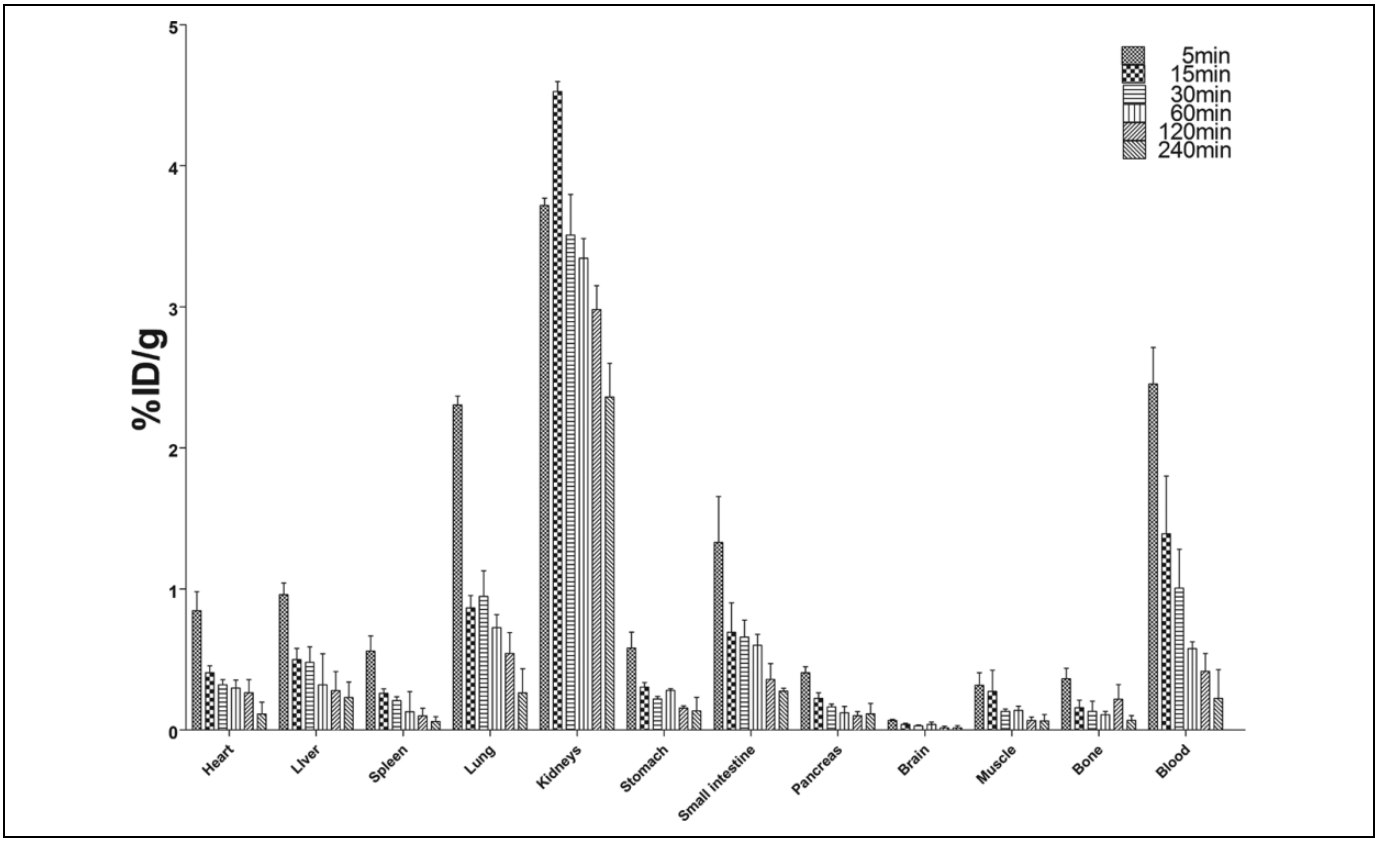

Figure 3. Biodistribution of ^{99m}Tc-duramycin in mice at 5, 15, 30, 60, 120, and 240 minutes (n = 3). Radioactivity was expressed as a percentage of the injected dose per gram of wet tissue (ID %/g).

findings were in line with the percentage of apoptotic cells detected by flow cytometric analysis, approximately 56% apoptosis was observed in the paclitaxel-treated cells, significantly higher than that of nontreated cells (2%).

Biodistribution and Clearance Kinetics in Balb/c Mice

^{99m}Tc-duramycin uptake by the main organs at various time points after intravenous injection is shown in Figure 3. The most predominant uptake was in the kidney, which gradually decreased with time, and the liver and spleen showed a comparatively lower uptake. Relatively little uptake of ^{99m}Tc-duramycin was observed in the heart and lung.

A 3-compartment model best described the blood clearance time profiles for ^{99m}Tc-duramycin in Balb/c mice. The half-life for the fast clearance phase (α-phase) was estimated to be 4.1 ± 0.3 minutes (n = 5) whereas that of the slow clearance phase (β-phase) was 171.6 ± 32.3 minutes. The radiotracer uptake in the blood at 120 minutes postinjection was 0.42 ± 0.13 ID%/g.

Response to Paclitaxel Treatment in MDA-MB-231 Tumor Xenografts

After 40 mg/kg paclitaxel treatment, the volume of tumor was calculated at day 0, day 3, day 5, and day 7. The vessels in the surface of tumor disappeared after treatment, tumor volume was 0.60 ± 0.09, 0.21 ± 0.05, 0.09 ± 0.03, 0.04 ± 0.01 cm^3, respectively, whereas tumor volume in untreated control was 0.59 ± 0.05, 1.03 ± 0.13, 1.96 ± 0.15, 2.95 ± 0.23 cm^3, respectively, at day 0, day 3, day 5, and day 7 (Figure 4). Tumor volume decreased significantly after paclitaxel on days 5 and day 7 ($P < .001$).

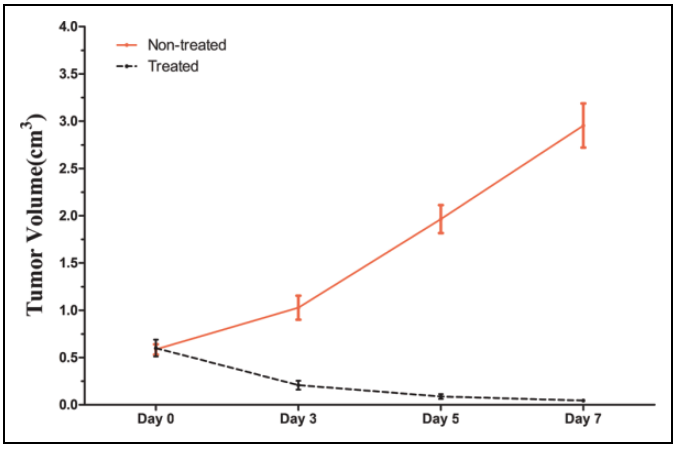

Figure 4. After paclitaxel treatment, the tumor volume decreased significantly, whereas the tumor grew continuously in the untreated group.

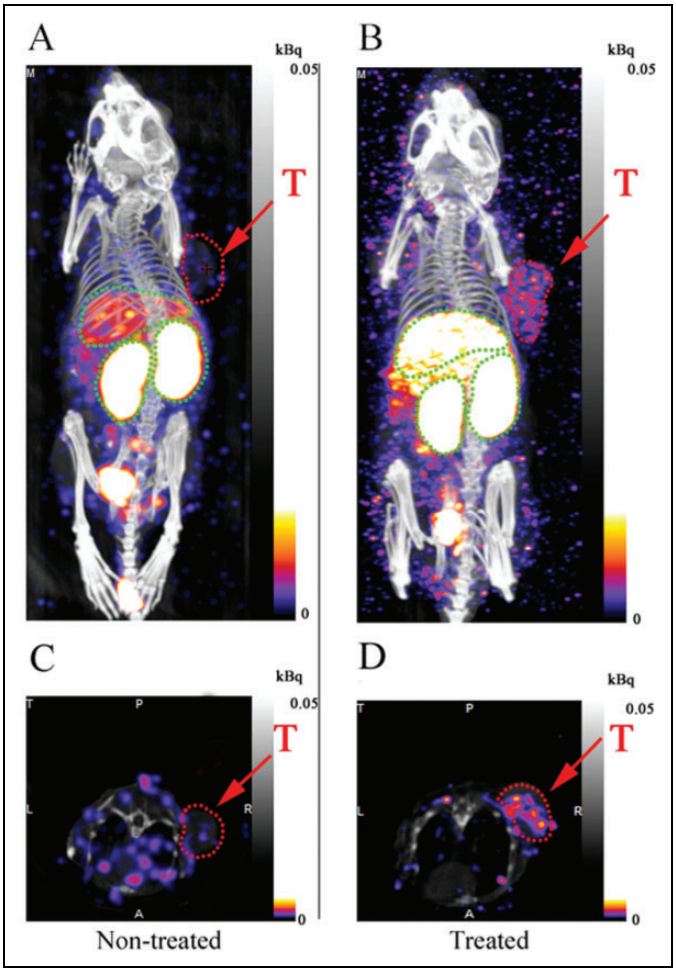

Figure 5. Representative Nano SPECT/computed tomography (CT) images of ^{99m}Tc-duramycin in MDA-MB-231 tumor xenografts in vivo. (A and C): Transverse and coronal images after treatment. (B and D): Corresponding image in untreated control. Tumor (T) is indicated by arrow.

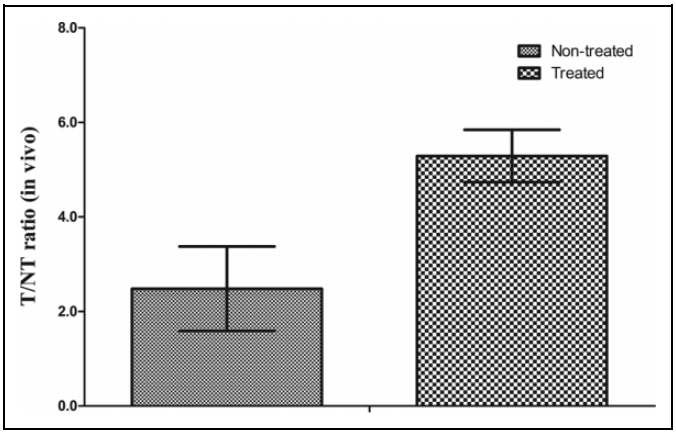

Figure 6. The ratio of tumor to contralateral normal tissue was analyzed in ^{99m}Tc-duramycin image. T/NT in the paclitaxel-treated mice was 5.29 $\pm$ 0.62, significantly higher than that in the control (2.48 $\pm$ 0.89, $P < .05$)

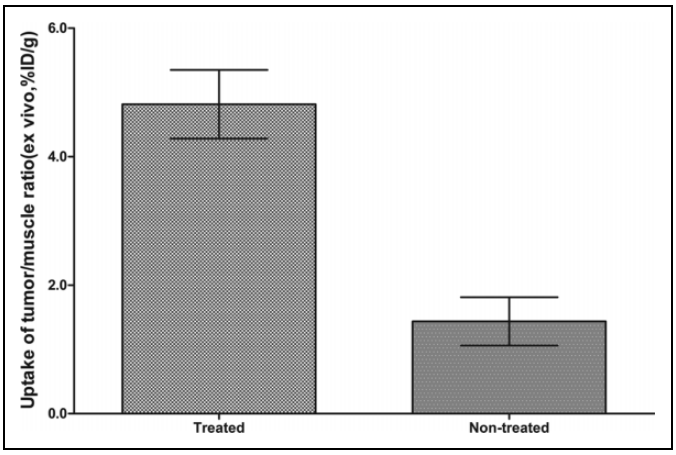

Figure 7. The ratio of tumor-to-muscle (T/NT) radio uptake (ID%/g) in the ex vivo biodistribution of ^{99m}Tc-duramycin. T/NT in paclitaxel-treated group was 4.81 $\pm$ 0.54, significantly higher than that of untreated tumors (1.44 $\pm$ 0.38, $P < .001$).

The SPECT/CT Imaging Analysis and ^{99m}Tc-Duramycin Ex Vivo Distribution in Tumor Xenografts

Representative Nano SPECT/CT images of ^{99m}Tc-duramycin uptake in MDA-MB-231 tumor xenografts are shown in Figure 5. The ROI analysis was performed for semiquantitation of radiotracer uptake and ^{99m}Tc-duramycin uptake (T/NT) in the untreated control, and paclitaxel-treated group was shown in Figure 6. The T/NT in the paclitaxel-treated mice was 5.29 $\pm$ 0.62, significantly higher than that in the control (2.48 $\pm$ 0.89, $P < .05$).

The ex vivo biodistribution of ^{99m}Tc-duramycin in treated tumor and untreated mice has been completed, the ratio of T/NT uptake (ID%/g) in paclitaxel-treated group was 4.81 $\pm$ 0.54, significantly higher than that of untreated tumors (1.44 $\pm$ 0.38, $P < .001$), as shown in Figure 7.

Histopathological Analysis: TUNEL Assay and TEM Analysis

Representative histological images are shown in Figure 8A-D. The H&E staining was shown in Figure 8A and B. DNA fragmentation was analyzed by TUNEL assay. The TUNEL-positive cells markedly exhibited cell shrinkage, condensed nuclei, and the appearance of apoptotic bodies (Figure 8C and D).

Ultrastructural changes associated with apoptosis was observed by TEM; the percentage of apoptotic cells was characterized by cell shrinkage and nuclear/chromatin condensation, and apoptotic bodies was higher in the paclitaxel-treated tumor tissues than that in the control (Figure 8E and F).

Quantitation of Activated Caspase 3 in Tumor Tissues

As it has been reported that necrotic cells and nuclei undergoing active gene transcription can be TUNEL positive, we evaluated the percentage of caspase 3-activated cells by flow cytometry to confirm the specificity of labeling of apoptotic

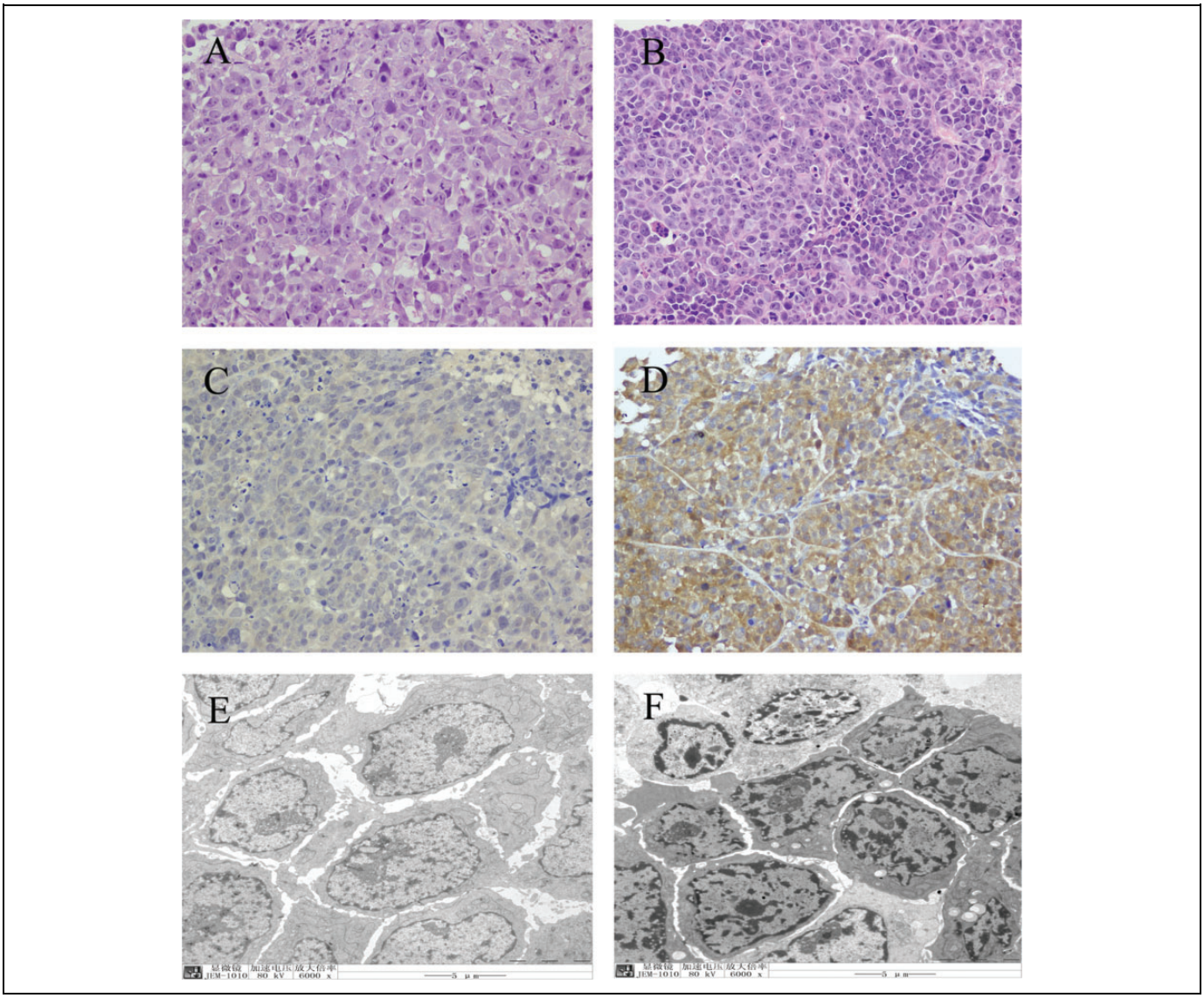

Figure 8. Representative images of the histological staining of tumor tissues and transmission electron microscopy (TEM), untreated tumor (A, C, and E), and paclitaexl-treated tumor (B, D, and F). (A and B) Hematoxylin and eosin staining (Original magnification ×400). (C and D) TUNEL staining (original magnification ×400). (E and F) Ultrastructural changes observed by TEM (original magnification ×6000).

Table 1. Comparison of T/NT Ratios of ^{99m}Tc-Duramycin, TUNEL-Positive Cells, and Activated Caspase 3 Levels in Tumor Tissues Between the Paclitaxel-Treated Group and the Control.[a]

Groups	T/NT	Activated Caspase 3	FITC-Annexin V/PI binding
Paclitaxel	5.29 ± 0.62[b]	53.04 ± 7.25[b]	46.80 ± 7.25[b]
Control	2.48 ± 0.89	11.49 ± 3.83	11.04 ± 5.44

Abbreviations: FITC, fluorescein isothiocyanate; SD, standard deviation; T/NT, tumor to muscle.
[a]Activated caspase-3 and FITC-annexin V levels were measured by flow cytometry. Data are presented as the mean percentage ± SD (n = 5).
[b]$P < .01$ versus control.

cells. As shown in Table 1, in line with the above-mentioned findings, activated caspase 3 in the paclitaxel-treated tissues (53.0% ± 7.3%) was found to be significantly higher than that in nontreated tissues (11.5% ± 3.8%; $P < .01$).

The FITC-Annexin V/PI Analysis

In the present study, apoptosis was quantified by bivariate FITC-annexin V/PI analysis using flow cytometry. Apoptosis can be detected via annexin V binding to phosphatidylethanolamine

(PE) at the cell surface of apoptotic cells. As depicted in Figure 2B and C, apoptotic cells were clearly visualized in the bivariate FITC-annexin V/PI analysis. Corroborating the results obtained in vitro, flow cytometric FITC-annexin V/PI analysis revealed a higher number of apoptotic cells in the paclitaxel-treated tumor tissues indicated by a higher apoptotic (annexin V+/PI−) population (46.8% ± 7.3%) when compared to the untreated tissues (11.0% ± 5.4%), which further implied that the uptake of ^{99m}Tc-duramycin in the paclitaxel-treated tumor tissues was higher than that of the control (Table 1).

Discussion

Breast cancer has been the second leading cause of mortality in woman worldwide.[26] The outcome of breast cancer is dependent upon the characteristics of tumor and the nature of treatment. Preoperative neoadjuvant chemotherapy has already been used as the standard treatment for inflammatory and nonoperable, locally advanced breast carcinoma and now increasingly being used for patients with operable but advanced breast tumors. This strategy allows patients to undergo breast-conserving surgery and provides information on the efficacy of chemotherapy.[27] Early response prediction after 1 or 2 cycles of neoadjuvant chemotherapy may enable the selection of alternative strategies. Paclitaxel as a first-line anticancer drug in breast carcinoma can induce tumor apoptosis and inhibition of microtubules movement.[28]

Molecular imaging approaches are rapidly emerging and hold promise in the clinical setting by enabling earlier lesion detection, treatment response monitoring, and tailoring of individualized therapy for patient benefit.[29] In the present study, we utilized ^{99m}Tc-labeled duramycin and SPECT/CT to monitor apoptosis in MDA-MB-231 breast carcinoma xenografts following paclitaxel treatment, and it was aimed to evaluate apoptosis after neoadjuvant chemotherapy using a radiolabeled PE-binding agent.[30]

A hallmark of apoptosis is the redistribution of phospholipid species across the bilayer of the plasma membrane. Both PE and PS are the predominant constituents of the inner leaflet of the plasma membrane. Because mammalian cellular membranes have much higher PE content, which is often several folds higher than the content of PS, exposure of PE is likely to further enhance the uptake of PE-specific agents, thus leading to higher signal intensity for apoptosis imaging.[31]

Duramycin is a 19-amino acid lantibiotic peptide produced by *Streptoverticillium cinnamoneus*, and it possesses a unique 3-dimensional structure with a low molecular weight (2 kDa). Structural analysis of duramycin revealed extensive intramolecular crosslinking that includes 1 lanthionine, 2 methyllanthionines, and 1 lysinoalanine, with no free peptide termini and a well-defined 3-dimensional binding pocket. Given its unique features such as a relatively low molecular weight, better biodistribution with a faster blood clearance, extreme structural stability, availability of N-terminal labeling, and a lower background, this PE-specific lantibiotic is thus a favorable molecular probe candidate for in vivo imaging applications.

In this study, ^{99m}Tc-duramycin had a purity higher than 90% and exhibited chemical and radiochemical stability without any dissociated radioactivity upon radiolabeling. Therefore, high radiochemical purity together with stability and easy preparation makes ^{99m}Tc-duramycin promising for various clinical applications.^{99m}Tc-duramycin showed suitable clearance and biodistribution profiles and could identify myocardial ischemia in porcine model in our latest study.[32] This study further verified ^{99m}Tc-duramycin with better biodistribution and notably enhanced pharmacokinetic profile in the xenograft of MDA-MB-231 breast tumor in vivo. Characteristics such as fast blood clearance and low hepatic background were identified as being of particular interest. Further, a 3-compartment model displayed the best fit to the blood clearance time profiles of ^{99m}Tc-duramycin, where the half-life for the fast clearance phase (α phase) was estimated to be 4.1 ± 0.3 minutes. The radiouptake in blood at 120 minutes postinjection was found to be 0.42 ± 0.13 ID%/g. These results indicate that ^{99m}Tc-duramycin with its better distribution had more merits for the detection of apoptosis.

The in vitro binding assay demonstrated a significantly higher radio uptake in paclitaxel-treated MDA-MB-231 cells (2.23 ± 0.32 folds) when compared to nontreated cells. The tumor volume decreased significantly, and the vessels in the surface of tumor disappeared after paclitaxel treatment. Ex vivo distribution demonstrated ^{99m}Tc-duramycin uptake in the tumor was significantly higher than that of untreated tumor. ^{99m}Tc-duramycin imaging showed focal uptake in the tumor after chemotherapy, whereas mild uptake in the control, and T/NT in paclitaxel-treated group was 5.29 ± 0.62, significantly higher than that in the control group (2.48 ± 0.89). This finding was consistent with ex vivo study in breast xenograft.

Apoptosis of neoplastic cells in response to therapy indicates successful treatment, and imaging of apoptosis could be a useful tool for early evaluation of the tumor response to therapy. Histopathological staining including TUNEL staining and ultramorphologic changes are the most widely used method to detect apoptosis. A large number of apoptotic cells, characterized by cell shrinkage, condensed nuclei, and the appearance of apoptotic bodies, were observed in the paclitaxel-treated tumor tissue specimens, and consistent results were further identified by TEM. Significant ongoing apoptosis induced by paclitaxel treatment resulted in significantly higher uptake of ^{99m}Tc-duramycin on the tumor, which indicated ^{99m}Tc-duramycin might serve as potential probe for the detection of apoptosis after neoadjuvant therapy.

It should be noted that there is a background uptake of ^{99m}Tc-duramycin in untreated tumors. This uptake could be attributed to at least 2 factors. First, according to ex vivo tissue analyses, the presence of apoptotic cells in untreated tumors was lower compared to posttreatment tumors but still significant relative to normal tissues (11.0% ± 5.4% by flow cytometry and 11.5% ± 3.8% by Caspase staining). Second, it has been reported that there is an elevated presence of PE in tumor

vascular endothelium, especially at or near hypoxic regions within the tumor.[33] As such, apart from an intrinsically higher apoptotic rate in untreated tumors, the presence of PE at vascular endothelium in these tumors may have contributed to the baseline signal prior to chemotherapy. After paclitaxel treatment, there were greater number of ongoing apoptotic cells in tumor when compared to the nontreated control. Interestingly, when in vivo imaging data are compared to the ex vivo tissue analyses, a discrepancy appears to exist between the elevation in radioactivity uptake from ^{99m}Tc-duramycin (2.23 folds increase) and the changes in percentages of apoptosis measured ex vivo (4.2-fold by flow cytometry and 4.6-fold by Caspase staining). This phenomenon can be at least in part explained by the nature of probe–target interactions in living tissues. After intravenous injection, the probe gains access to the binding targets via blood circulation. It is conceivable that blood perfusion and probe extravasation from the vasculature can have a significant impact on probe accessibility to its binding targets. In contrast, histopathology involves tissue cross sections, where every single cell within the cross section is fully exposed to staining reagents.

Overall, the present study demonstrated that the ^{99m}Tc-duramycin uptake in the tumor significantly increased following paclitaxel treatment, which in turn was correlated with the apoptotic index, histological findings, ultrastructural changes, and bivariate FITC-Annexin V-flow cytometric results. These data suggest the feasibility of using ^{99m}Tc-duramycin for early detection of apoptosis after paclitaxel treatment.

Conclusion

Our data demonstrate the feasibility of ^{99m}Tc-duramycin for the early detection of apoptosis after paclitaxel chemotherapy in breast tumor xenografts. ^{99m}Tc-duramycin may serve as a potential apoptosis imaging probe because of its avid target binding, rapid blood clearance, and low liver uptake and thus aid in the evaluation of the response to tumor treatment. This study may shed light on early evaluation and neoadjuvant therapy-induced apoptosis. Further studies in various preclinical models of apoptosis are needed to define the clinical utilization of this molecular probe.

Author's Note

Rui Luo and Lei Niu contributed equally to the article.

Declaration of Conflicting Interests

The author(s) declared no potential conflicts of interest with respect to the research, authorship, and/or publication of this article.

Funding

The author(s) disclosed receipt of the following financial support for the research, authorship, and/or publication of this article: This research was supported by grants from National Natural Science Foundation of China (81271604, 81171383, 81071176), Jiangsu Provincial Nature Science Foundation (BL2012037, BK2011104), and the National Institute of Health (R01 HL102085, 5R01CA185214).

References

1. Michaelis LC, Ratain MJ. Measuring response in a post-RECIST world: from black and white to shades of grey. *Nat Rev Cancer*. 2006;6(5):409-414.
2. Goffin J, Baral S, Tu D, Nomikos D, Seymour L. Objective responses in patients with malignant melanoma or renal cell cancer in early clinical studies do not predict regulatory approval. *Clin Cancer Res*. 2005;11(16):5928-5934.
3. Dubray B, Breton C, Delic J, et al. In vitro radiation-induced apoptosis and early response to low-dose radiotherapy in non-Hodgkin's lymphomas. *Radiother Oncol*. 1998;46(2):185-191.
4. Chang J, Ormerod M, Powles TJ, Allred DC, Ashley SE, Dowsett M. Apoptosis and proliferation as predictors of chemotherapy response in patients with breast carcinoma. *Cancer*. 2000; 89(11):2145-2152.
5. Ellis PA, Smith IE, McCarthy K, Detre S, Salter J, Dowsett M. Preoperative chemotherapy induces apoptosis in early breast cancer. *Lancet*. 1997;349(9055):849.
6. Kartachova M, van Zandwijk N, Burgers S, van Tinteren H, Verheij M, Valdés Olmos RA. Prognostic significance of ^{99m}TcHynic-rh-annexin V scintigraphy during platinum-based chemotherapy in advanced lung cancer. *J Clin Oncol*. 2007; 25(18):2534-2539.
7. Kartachova MS, Valdés Olmos RA, Haas RL, Hoebers FJ, van Herk M, Verheij M. 99mTc-HYNIC-rh-annexin-V scintigraphy: visual and quantitative evaluation of early treatment-induced apoptosis to predict treatment outcome. *Nucl Med Commun*. 2008;29(1):39-44.
8. van de Wiele C, Lahorte C, Vermeersch H, et al. Quantitative tumor apoptosis imaging using technetium-99m-HYNIC annexin V single photon emission computed tomography. *J Clin Oncol*. 2003;21(18):3483-3487.
9. Haas RL, de Jong D, Valdés Olmos RA, et al. In vivo imaging of radiation-induced apoptosis in follicular lymphoma patients. *Int J Radiat Oncol Biol Phys*. 2004;59(3):782-787.
10. Rottey S, Slegers G, Van Belle S, Goethals I, Van de Wiele C. Sequential 99mTc-hydrazinonicotinamide-annexin V imaging for predicting response to chemotherapy. *J Nucl Med*. 2006;47(11): 1813-1818.
11. Wang F, Fang W, Zhao M, et al. Imaging paclitaxel (chemotherapy)-induced tumor apoptosis with 99mTc C2A, a domain of Synaptotagmin I: a preliminary study. *Nucl Med Biol*. 2008; 35(3):359-364.
12. Wang F, Fang W, Zhang MR, et al. Evaluation of chemotherapy response in VX2 rabbit lung cancer with 18F-labeled C2A domain of synaptotagmin I. *J Nucl Med*. 2011;52(4):592-599.
13. Benali K, Louedec L, Azzouna RB, et al. Preclinical validation of 99mTc-annexin A5-128 in experimental autoimmune myocarditis and infective endocarditis: comparison with 99mTc-HYNIC-annexin A5. *Mol Imaging*.2014:13.
14. Bevers EM, Comfurius P, Dekkers DW, Zwaal RF. Lipid translocation across the plasma membrane of mammalian cells. *Biochim Biophys Acta*. 1999;1439(3):317-330.
15. Daleke DL. Regulation of transbilayer plasma membrane phospholipid asymmetry. *J Lipid Res*. 2003;44(2):233-242.

16. Williamson P, Schlegel RA. Transbilayer phospholipid movement and the clearance of apoptotic cells. *Biochim Biophys Acta*. 2002;1585(2-3):53-63.
17. Emoto K, Toyama-Sorimachi N, Karasuyama H, Inoue K, Umeda M. Exposure of phosphatidylethanolamine on the surface of apoptotic cells. *Exp Cell Res*. 1997;232(2):430-434.
18. Hayashi F, Nagashima K, Terui Y, Kawamura Y, Matsumoto K, Itazaki H. The structure of PA48009: the revised structure of duramycin. *J Antibiot (Tokyo)*. 1990;43(11): 1421-1430.
19. Zimmermann N, Freund S, Fredenhagen A, Jung G. Solution structures of the lantibiotics duramycin B and C. *Eur J Biochem*. 1993;216(2):419-428.
20. Zhao M, Li Z, Bugenhagen S. ^{99m}Tc-labeled duramycin as a novel phosphatidylethanolamine-binding molecular probe. *J Nucl Med*. 2008;49(8):1345-1352.
21. Audi S, Li Z, Capacete J, et al. Understanding the in vivo uptake kinetics of a phosphatidylethanolamine-binding agent (99 m)Tc-Duramycin. *Nucl Med Biol*. 2012;39(6):821-825.
22. Zhao M, Li Z. A single-step kit formulation for the (99 m)Tc-labeling of HYNIC-Duramycin. *Nucl Med Biol*. 2012;39(7): 1006-1011.
23. Johnson SE, Li Z, Liu Y, Moulder JE, Zhao M. Whole-body imaging of high-dose ionizing irradiation-induced tissue injuries using 99mTc-duramycin. *J Nucl Med*. 2013;54(8): 1397-403.
24. Audi SH, Jacobs ER, Zhao M, Roerig DL, Haworth ST, Clough AV. In vivo detection of hyperoxia-induced pulmonary endothelial cell death using (99 m)Tc-Duramycin. *Nucl Med Biol*. 2015;42(1):46-52.
25. Madar I, Huang Y, Ravert H, et al. Detection and quantification of the evolution dynamics of apoptosis using the PET voltage sensor 18F-fluorobenzyl triphenyl phosphonium. *J Nucl Med*. 2009; 50(5):774-780.
26. Jemal A, Siegel R, Ward E, Murray T, Xu J, Thun MJ. Cancer statistics, 2007. *CA Cancer J Clin*. 2007;57(1):43-66.
27. Bear HD, Tang G, Rastogi P, et al. Neoadjuvant chemotherapy and bevacizumab for HER2-negative breast cancer. *N Engl J Med*. 2012;366(4):310-320.
28. Sparano J. A., Wang M., et al. Weekly paclitaxel in the adjuvant treatment of breast cancer. *N Engl J Med*. 2008;358(16):1663-1671.
29. Michalski M H, Chen X. Molecular imaging in cancer treatment. *Eur J Nucl Med Mol Imaging*. 2011;38(2):358-377.
30. Yao S, Hu K, Tang G, et al. Positron emission tomography imaging of cell death with [18F]FPDuramycin. *Apoptosis*. 2014; 19(5):841-850.
31. Vance JE. Phosphatidylserine and phosphatidylethanolamine in mammalian cells: two metabolically related aminophospholipids. *J Lipid Res*. 2008;49(7):1377-1383.
32. Wang L, Wang F, Fang W, et al. The feasibility of imaging myocardial ischemic/reperfusion injury using 99mTc-labeled duramycin in a porcine model. *Nucl Med Biol*. 2015;42(2): 198-204.
33. Stafford JH, Thorpe PE. Increased exposure of phosphatidylethanolamine on the surface of tumor vascular endothelium. *Neoplasia*. 2011;13(4):299-308.